diabetes®

American Diabetes Association®

Hematopoietic NLRP3 and AIM2 Inflammasomes Promote Diabetes-Accelerated Atherosclerosis, but Increased Necrosis Is Independent of Pyroptosis

Cheng-Chieh Hsu, Trevor P. Fidler, Jenny E. Kanter, Vishal Kothari, Farah Kramer, Jingjing Tang, Alan R. Tall, and Karin E. Bornfeldt

Diabetes 2023;72(7):999–1011 | https://doi.org/10.2337/db22-0962

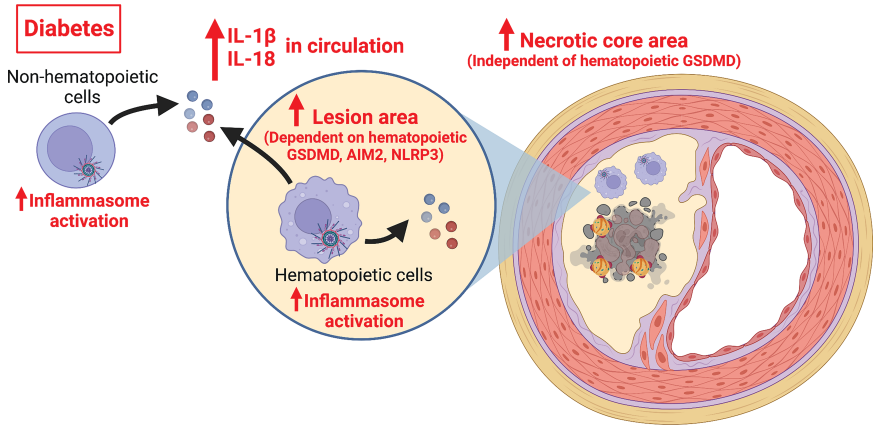

Hematopoietic NOD, LRR, and pyrin domain-containing protein 3 (NLRP3) and absent in melanoma 2 (AIM2) inflammasomes promote diabetes-accelerated atherosclerosis, but increased necrosis is independent of pyroptosis. GSDMD, gasdermin D; IL, interleukin.

Hematopoietic NLRP3 and AIM2 Inflammasomes Promote Diabetes-Accelerated Atherosclerosis, but Increased Necrosis Is Independent of Pyroptosis

Cheng-Chieh Hsu,[1] Trevor P. Fidler,[2] Jenny E. Kanter,[1] Vishal Kothari,[1] Farah Kramer,[1] Jingjing Tang,[1] Alan R. Tall,[2] and Karin E. Bornfeldt[1]

Diabetes 2023;72:999–1011 | https://doi.org/10.2337/db22-0962

Serum apolipoprotein C3 (APOC3) predicts incident cardiovascular events in people with type 1 diabetes, and silencing of APOC3 prevents both lesion initiation and advanced lesion necrotic core expansion in a mouse model of type 1 diabetes. APOC3 acts by slowing the clearance of triglyceride-rich lipoproteins, but lipid-free APOC3 has recently been reported to activate an inflammasome pathway in monocytes. We therefore investigated the contribution of hematopoietic inflammasome pathways to atherosclerosis in mouse models of type 1 diabetes. LDL receptor–deficient diabetes mouse models were transplanted with bone marrow from donors deficient in NOD, LRR and pyrin domain–containing protein 3 (NLRP3), absent in melanoma 2 (AIM2) or gasdermin D (GSDMD), an inflammasome-induced executor of pyroptotic cell death. Mice with diabetes exhibited inflammasome activation and consistently, increased plasma interleukin-1β (IL-1β) and IL-18. Hematopoietic deletions of NLRP3, AIM2, or GSDMD caused smaller atherosclerotic lesions in diabetic mice. The increased lesion necrotic core size in diabetic mice was independent of macrophage pyroptosis because hematopoietic GSDMD deficiency failed to prevent necrotic core expansion in advanced lesions. Our findings demonstrate that AIM2 and NLRP3 inflammasomes contribute to atherogenesis in diabetes and suggest that necrotic core expansion is independent of macrophage pyroptosis.

ARTICLE HIGHLIGHTS

- The contribution of hematopoietic cell inflammasome activation to atherosclerosis associated with type 1 diabetes is unknown.
- The goal of this study was to address whether hematopoietic NOD, LRR, and pyrin domain–containing protein 3 (NLRP3), absent in melanoma 2 (AIM2) inflammasomes, or the pyroptosis executioner gasdermin D (GSDMD) contributes to atherosclerosis in mouse models of type 1 diabetes.
- Diabetic mice exhibited increased inflammasome activation, with hematopoietic deletions of NLRP3, AIM2, or GSDMD causing smaller atherosclerotic lesions in diabetic mice, but the increased lesion necrotic core size in diabetic mice was independent of macrophage pyroptosis.
- Further studies on whether inflammasome activation contributes to cardiovascular complications in people with type 1 diabetes are warranted.

Despite the success of statins in reducing cardiovascular disease (CVD) events (1), CVD remains the leading cause of death in the U.S. (1). Numerous efforts have been made to reduce CVD mortality, but the trend has stalled, in part because of the rising prevalence of diabetes (1). Individuals with type 1 or type 2 diabetes have an increased risk of atherosclerotic CVD (1). The persistently elevated CVD risk among individuals with diabetes, despite lowering LDL, suggests the presence of residual risks. Multiple risk factors, including glucose (2,3), inflammation (4,5), and abnormal metabolism of triglyceride-rich lipoproteins

[1]Division of Metabolism, Endocrinology and Nutrition, Department of Medicine, University of Washington Medicine Diabetes Institute, University of Washington, Seattle, WA
[2]Division of Molecular Medicine, Department of Medicine, Columbia University Irving Medical Center, New York, NY

Corresponding author: Karin E. Bornfeldt, bornf@uw.edu

Received 18 November 2022 and accepted 15 April 2023

This article contains supplementary material online at https://doi.org/10.2337/figshare.22659121.

(TRLs) and their remnants (6–8), have been proposed as contributors to residual risk.

Monocytes and macrophages play important roles in all stages of atherosclerotic lesion development (5,9). The accumulation of monocytes in response to lipoprotein accumulation in the artery wall and their subsequent differentiation into macrophages exacerbate arterial inflammation (10). Macrophages can undergo programmed cell death after taking up lipoproteins, contributing to the lipid-rich, acellular necrotic cores that characterize the progression of the advanced lesion (9,10). Individuals with diabetes have increased lesional macrophage content (based on $CD68^+$ immunoreactivity) and necrotic cores that could contribute to the acceleration of atherosclerosis (11) and CVD events (12). With the Canakinumab Anti-inflammatory Thrombosis Outcome Study (CANTOS) highlighting the causal involvement of interleukin-1β (IL-1β) in atherosclerotic cardiovascular events in individuals with and without diabetes (13), the roles of macrophages and inflammation, especially the inflammasome pathways responsible for the secretion of mature IL-1β and IL-18, in diabetes-associated atherosclerosis have gained intense interest.

Apolipoprotein C3 (APOC3) has been reported to predict future CVD events in individuals with type 1 diabetes from three different cohorts (14–16). Although APOC3 likely exacerbates diabetes-associated atherosclerosis primarily via inhibiting the clearance of TRLs and their remnants (7), lipid-free APOC3 has been shown to activate an alternative inflammasome pathway in human and mouse monocytes (17,18).

The findings above, together with a report demonstrating that individuals with type 2 diabetes have elevated serum levels of IL-1β and IL-18 (19), make it tempting to speculate that inflammasome pathways could contribute to atherosclerosis and clinical events in individuals with diabetes and that inflammasome inhibition might be beneficial in diabetes. Furthermore, statins can increase the incidence of type 2 diabetes through a mechanism that may involve inflammasome activation (20,21). Hematopoietic deficiencies in essential inflammasome components, such as NOD, LRR, and pyrin domain–containing protein 3 (NLRP3) (22–24), absent in melanoma 2 (AIM2) (25), apoptosis-associated speck-like protein containing a CARD (ASC) (24), or caspase-1/11 (22), have been reported to be atheroprotective in mice with diseases that promote inflammasome activation. Moreover, a recent study demonstrated that systemic inhibition of the NLRP3 pathway using the small-molecule NLRP3 inhibitor MCC950 is atheroprotective in diabetic APOE–deficient mice (4). However, whether inflammasome components contribute to diabetes-associated atherosclerosis via the hematopoietic compartment remains unexplored.

Upon activation of NLRP3 or AIM2 inflammasomes, activated caspase-1 cleaves pro-IL-1β and pro-IL-18 into their mature forms, which are secreted upon caspase-1 activation of the pore-forming protein gasdermin D (GSDMD) (26). GSDMD activation also promotes proinflammatory cell death, called pyroptosis (26). Consistent with the studies demonstrating that inflammasome pathways contribute to atherosclerosis, global GSDMD deficiency has been reported to be atheroprotective in some studies (27) but not others (25) in LDL receptor–deficient ($Ldlr^{-/-}$) mice. It is not known whether similar mechanisms contribute to diabetes-accelerated atherosclerosis.

To address whether hematopoietic inflammasome activation and pyroptosis contribute to diabetes-associated atherosclerosis, we investigated the role of hematopoietic GSDMD, AIM2, and NLRP3. We demonstrate that diabetes is associated with inflammasome activation and elevated plasma IL-1β and IL-18. Furthermore, while both hematopoietic NLRP3 and AIM2 inflammasomes and GSDMD contributed to lesion development in diabetic mice, the necrotic core expansion could not be explained by macrophage pyroptosis mediated by GSDMD, as hematopoietic GSDMD deficiency failed to provide protection.

RESEARCH DESIGN AND METHODS

Mouse Models

All animal studies were approved by the institutional animal care and use committees of the University of Washington and Columbia University.

Virus-Induced Mouse Model of Type 1 Diabetes-Accelerated Atherosclerosis

As described previously (28), $Ldlr^{-/-}$ mice expressing the lymphocytic choriomeningitis virus (LCMV) glycoprotein transgene (Gp^{Tg}) under control of the rat insulin promoter, allowing reliable induction of $CD8^+$ T-cell–mediated β-cell destruction upon LCMV injection (Armstrong 53b; 1.3×10^4 plaque-forming units/mouse), were used as one of the mouse models of type 1 diabetes–accelerated atherosclerosis. Littermates without the glycoprotein transgene (Gp^0) were used for evaluating the possible effects of LCMV independent of diabetes. Female mice were used in this study because the NLRP3 inflammasome pathway has been reported to play a more important role in atherosclerosis in female mice than in male mice (29).

For the study on plasma analytes, 8- to 12-week-old female $Ldlr^{-/-}$;Gp^{Tg} and $Ldlr^{-/-}$;Gp^0 mice on a C57BL/6J background were injected with LCMV (Armstrong 53b; 1.3×10^4 plaque-forming units/mouse) to serve as the diabetic group and virus control group. Nondiabetic littermates received saline. After the onset of diabetes, defined by blood glucose >13.9 mmol/L, animals received insulin pellets (LinShin Canada Inc.) to provide baseline insulin and liquid insulin injections (Lantus) as needed to prevent ketonuria and severe weight loss. The mice were maintained on a low-fat diet (LFD) described previously (28) for 4 weeks before the termination of the study.

For the atherosclerosis studies, 6- to 10-week-old female $Ldlr^{-/-}$;Gp^{Tg} mice on a C57BL/6J background were maintained on a semipurified high-fat diet (HFD) for 12 weeks to allow the formation of preexisting atherosclerosis lesions and to allow us to study the effect of diabetes and

GSDMD on advanced lesions without confounding effects on lesion initiation. The HFD contained 40% fat and 1.25% added cholesterol (28). After 12 weeks of an HFD, the mice were switched to chow diet to normalize plasma lipid levels before being irradiated with 10 Gy from a cesium γ-source and receiving 5×10^6 bone marrow cells/recipient harvested from mice with and without GSDMD deficiency. The donor mice with clustered regularly interspaced short palindromic repeats–edited GSDMD deficiency (30) were provided by Genentech. The mice recovered for 5 weeks on a chow diet before induction of diabetes with LCMV. After the onset of diabetes, animals were maintained on an LFD for 4 weeks before the termination of the study, according to a published study design (31).

Mouse Model of Acute Inflammasome Activation

Eight- to 12-week-old female and male *Gsdmd*$^{-/-}$, *Gsdmd*$^{+/+}$, *Ldlr*$^{-/-}$;*Gp*^{Tg}, and C57BL/6J mice received an i.p. injection of 5 μg ultrapure lipopolysaccharide (LPS) (List Laboratories) or saline. Four hours after the first injection, animals received an i.p. injection of 5 mmol/L ATP or PBS. The experiment was terminated 1 h after the second injection. To investigate the role of hematopoietic GSDMD in IL-18 and IL-1β release following inflammasome activation, 8- to 12-week-old male *Ldlr*$^{-/-}$ mice received bone marrow harvested from mice with and without GSDMD deficiency. After a 5-week recovery on a chow diet, the mice received ultrapure LPS and ATP injections. Solutions were sterile filtered before the injections.

Streptozotocin-Induced Type 1 Diabetes Mouse Model

Eight- to 10-week-old female *Ldlr*$^{-/-}$ mice on a C57BL/6J background were irradiated with 10.5 Gy from a cesium γ-source and received 4×10^6 bone marrow cells/recipient harvested from female *Nlrp3*$^{-/-}$ (021302; The Jackson Laboratory) mice, *Aim2*$^{-/-}$ (013144; The Jackson Laboratory) mice, mice with double deficiencies of *Nlrp3* and *Aim2* (DKOs), or control wild-type mice. Mice recovered for 4 weeks on a chow diet before streptozotocin (STZ) injection (50 mg/kg i.p., 5 consecutive days) and were then switched to a Western diet (TD.88137; Envigo) for 8 weeks before the termination of the experiment.

Atherosclerosis Study in Whole-Body GSDMD-Deficient Mouse Model

Eight- to 12-week-old male mice with whole-body GSDMD deficiency and wild-type littermate controls on a C57BL/6 background were maintained on a high-fat, high-sucrose diet with added cholesterol (HFHS), as described previously (32), for 16 weeks before the termination of the experiment. While the mice were maintained on the HFHS diet, they received weekly i.p. injections of a GalNAc-conjugated LDLR antisense oligonucleotide (ASO) (5 mg/kg; Ionis Pharmaceuticals).

Genotyping

Genotyping for *Ldlr*, *Nlrp3*, and *Aim2* was conducted by following the manufacturer's protocols (The Jackson Laboratory). *Gsdmd* genotyping information is available in Supplementary Fig. 1.

Analysis of Blood Glucose and Plasma Analytes

Blood glucose levels were measured with a glucometer (OneTouch Ultra; LifeScan). Any values >33.3 mmol/L were reported as 33.3 mmol/L, as they reached the maximum detection limit of the device. Plasma analytes were measured with respective assays or kits described in Supplementary Table 1.

Quantification of Atherosclerosis

The aortas were dissected after perfusion with PBS and fixed with 10% phosphate-buffered formalin. The aortas were opened longitudinally and stained with Sudan IV as previously described (14,28). The aortic sinuses were fixed with 10% phosphate-buffered formalin, paraffin embedded, then serially sectioned for histological analysis. The sinus sections were stained with Movat pentachrome stain or hematoxylin and eosin to visualize lesion morphology. The sinuses were analyzed at three different sites, beginning at the appearance of all three aortic valve leaflets, using ImageJ software. Lesional Mac2, α-SMA, APOC3, APOB, and APOE immunoreactivity was determined by immunofluorescence. Stained samples were cover slipped with DAPI-containing mounting medium (Vector Laboratories) before imaging and quantifying with a fluorescence microscope (BZ-X800; Keyence). Lesion severity was analyzed according to the scoring system described by Stary et al. (33) as follows: 0 = no lesion, 1 = intimal change only (matrix), 2 = fatty streak without dramatic matrix expansion, 3 = fatty streaks with cholesterol clefts (extracellular lipids), 4 = lesions with necrotic cores, 5 = lesions with necrotic cores and abundant matrix, and 6 = ruptured lesions. The scores were summarized for each mouse. Investigators were blinded to the treatment groups during the processing and analysis of the samples. Costained areas were quantified before the single-stained areas. Details on the antibodies and negative controls are available in Supplementary Table 2 and Supplementary Figs. 2 and 3.

Flow Cytometry Analysis of Blood Leukocytes

Blood leukocyte populations were analyzed by flow cytometry and a gating strategy determined using single-stained and unstained controls (Supplementary Fig. 4 and Supplementary Table 3). Details on the antibodies are available in Supplementary Table 4.

Immunoblotting

Peritoneal cavity cells were harvested immediately with cold EDTA-containing PBS after experiment termination. A protease and phosphatase inhibitor cocktail (Thermo Fisher Scientific) was added immediately after sample collection. The samples were centrifuged at 400*g* for 5 min at 4°C to isolate peritoneal cavity cells and fluid. Peritoneal cavity cells were purified with an F4/80 Positive Selection Kit (Thermo Fisher Scientific) to enrich the macrophage population,

according to the manufacturer's instructions. Enriched F4/80$^+$ peritoneal cavity cells were lysed with radioimmunoprecipitation assay buffer (Thermo Fisher Scientific) containing a protease and phosphatase inhibitor cocktail. Samples were separated with SDS-PAGE and transferred to nitrocellulose membranes. Membranes were probed with primary and secondary antibodies before imaging (LI-COR). Antibody information is available in Supplementary Table 5.

Statistical Analysis

Power calculations were used to determine the number of animals per group. Investigators were blinded to the treatment groups during sample processing and data analysis. Statistical analyses were performed using GraphPad Prism 9.4.0 (GraphPad Software). Normality tests were performed using the D'Agostino and Pearson test. Data are displayed as mean ± SEM. Based on the normality of the data, the data were analyzed with two-sided Mann-Whitney *U* test, Kruskal-Wallis test, and Dunn multiple comparisons tests or with two-way ANOVA followed by Tukey multiple comparisons test. $P < 0.05$ was considered statistically significant. Statistical outliers were identified by Grubb test with $\alpha = 0.01$. All removed statistical outliers are described in the figure legends.

Data and Resource Availability

The data sets generated and/or analyzed during the current study are available from the corresponding author upon reasonable request. No applicable resources were generated or analyzed during the current study.

RESULTS

Diabetes Elevates Plasma Triglycerides, APOC3, and Inflammasome Signatures

To investigate whether diabetes activates inflammasome pathways, $Ldlr^{-/-}$;Gp^{Tg} mice were injected with saline or LCMV and maintained on an LFD for 4 weeks (Fig. 1*A*). The Gp^{Tg} animals had elevated levels of blood glucose after LCMV injection compared with those that received saline injections (Fig. 1*B*). Animals with blood glucose >13.9 mmol/L were considered diabetic. To verify that the effects of LCMV were due to diabetes and not only the LCMV, a virus control group ($Ldlr^{-/-}$;Gp^{0}) was included (Fig. 1*A*). Because of the lack of the Gp^{Tg} in β-cells, animals from the virus control group did not develop diabetes upon LCMV injection (Fig. 1*B*). Compared with nondiabetic animals, diabetic animals demonstrated elevated levels of plasma triglycerides, IL-18, IL-1β, and APOC3 (Fig. 1*C*–*G*). Consistent with the previous study by Zewinger et al. (17), elevated plasma APOC3 was accompanied by elevated plasma IL-18 and IL-1β, suggesting that activation of an inflammasome pathway in diabetic mice could be related to elevated levels of APOC3. Moreover, cleaved caspase-1 and the ratio of cleaved caspase-1 over full-length caspase-1 were elevated in the peritoneal cavity fluid from diabetic animals (Fig. 1*H*–*J*), further indicating inflammasome activation. Monocytosis and increased numbers of Ly6C^{high} monocytes, which have been suggested to contribute to atherosclerosis (34,35), were not observed in this mouse model of type 1 diabetes (Supplementary Table 3). The animals in the virus control group did not have these analytes elevated compared with the nondiabetic animals. The phenotypes of diabetic mice are therefore unlikely to be confounded by LCMV.

Hematopoietic GSDMD Reduces Lesion Area but Does Not Affect Atherosclerosis Lesion Phenotypes in Diabetic Mice

To investigate whether diabetes accelerates the progression of preexisting atherosclerotic lesions via a hematopoietic GSDMD-dependent pathway, female $Ldlr^{-/-}$;Gp^{Tg} mice with preexisting lesions received bone marrow transplants from animals with or without GSDMD deficiency before being rendered diabetic for 4 weeks (Fig. 2*A*). A subset of animals was euthanized before diabetes induction to evaluate the effects of genotypes on bone marrow reconstitution efficiency and lesion morphologies. Bone marrow GSDMD-deficient chimeras exhibited a 95–98% reconstitution in the blood, spleen, or peritoneal cavity (Supplementary Fig. 5A). Concurrently, hematopoietic deletion of GSDMD did not affect lesion morphologies at baseline prior to induction of diabetes (Supplementary Fig. 5*B*–*I*). After 4 weeks of an LFD, compared with nondiabetic animals, diabetic animals demonstrated elevated levels of blood glucose, plasma triglycerides, cholesterol, IL-18, IL-1β, and APOC3 (Fig. 2*B*–*G*), consistent with the short-term study (Fig. 1). However, hematopoietic GSDMD deficiency did not alter these levels. Current dogma predicts that myeloid cells are the major source of IL-1β and IL-18 released upon inflammasome and GSDMD activation (26). However, our findings suggest that plasma IL-1β and IL-18 are secreted by hematopoietic cells independently of GSDMD or are secreted by nonhematopoietic cells.

Although plasma IL-18 and IL-1β were not suppressed by hematopoietic GSDMD deficiency in mice with diabetes, we reasoned that GSDMD-mediated pyroptosis could contribute to atherosclerosis progression and necrotic core expansion. Similar to our previous studies (14,31) and a study in people (11), aortic sinus necrotic core size was exacerbated by diabetes without an effect on the size of preexisting sinus lesions (Fig. 2*H* and *I*) and aortic en face Sudan IV area (Supplementary Fig. 6*A*–*C*). Hematopoietic GSDMD deficiency resulted in smaller lesions in diabetic mice but did not alter necrotic core size in these mice (Fig. 2*H* and *I*). The lack of effects of the hematopoietic GSDMD deficiency on necrotic core size was not due to differences in monocytosis or accumulation of lesional macrophages (quantified by Mac2$^+$ immunoreactivity) or smooth muscle cells (quantified by α-SMA$^+$ immunoreactivity) (Supplementary Tables 6 and 7 and Supplementary Fig. 7). The lack of protective effects in this study suggest that diabetes exacerbates necrotic core expansion via mechanisms independent of hematopoietic GSDMD. We can only speculate on the reason behind the increased necrotic core area in nondiabetic mice

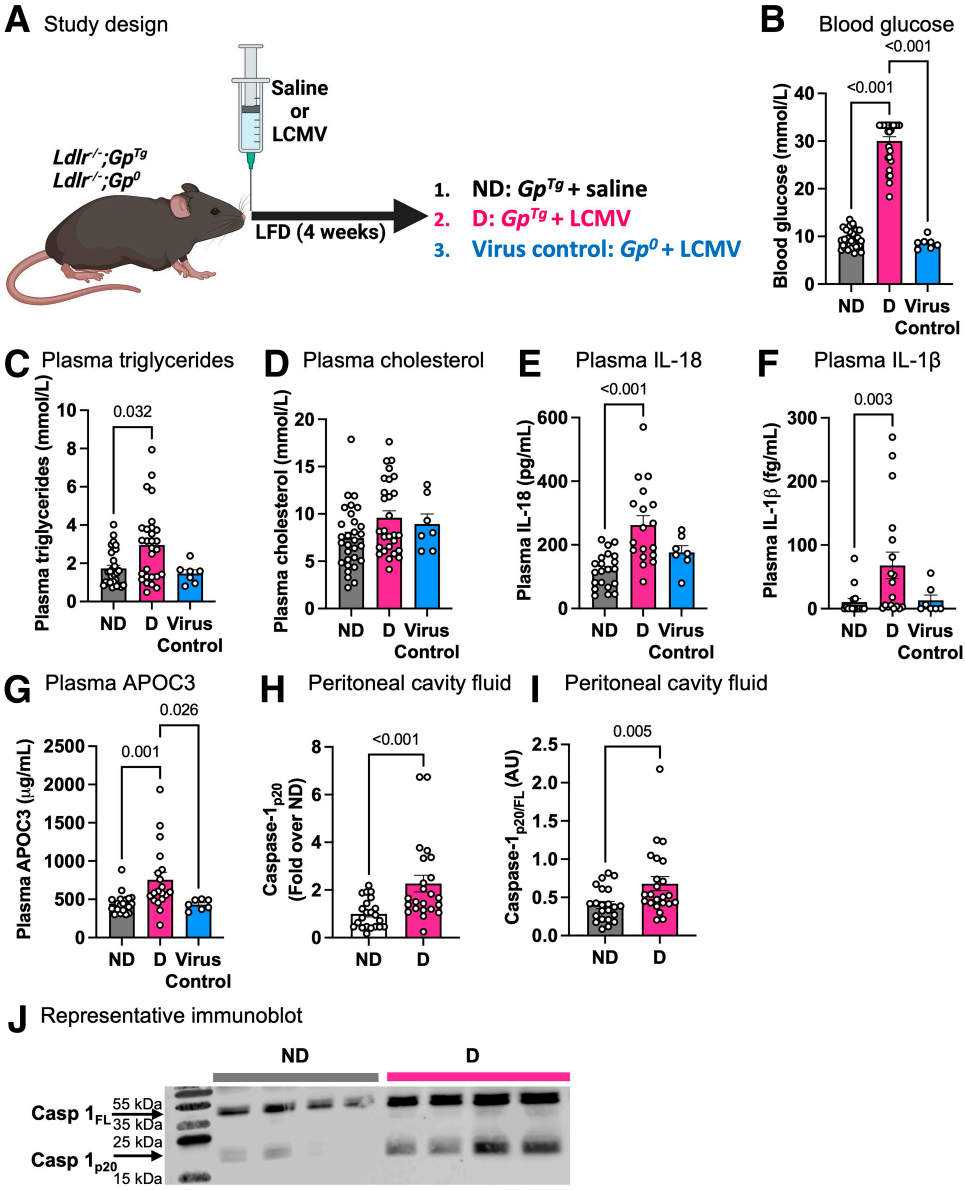

Figure 1—Diabetes leads to elevated plasma triglycerides, APOC3, and inflammasome signatures. Female *Ldlr*$^{-/-}$;*Gp*^{Tg} mice were rendered diabetic (D) with LCMV. Saline was used as a control (nondiabetic [ND]). *Ldlr*$^{-/-}$;*Gp*^{0} mice were injected with LCMV as a virus control. At the onset of diabetes, the animals were switched to a semipurified LFD with no added cholesterol and maintained for 4 weeks. *A*: Schematic of the study design. *B*: Blood glucose levels. Glucose values >33.3 mmol/L are expressed as 33.3 mmol/L. *C*: Plasma triglyceride levels. *D*: Plasma cholesterol levels. *E*: Plasma IL-18 levels. *F*: Plasma IL-1β levels. *G*: Plasma APOC3. *H* and *I*: Peritoneal cavity fluid was immunoblotted for cleaved caspase-1 (Casp 1_{p20}) and cleaved caspase-1 over full-length caspase-1 (Casp 1_{p20}/Casp 1_{FL}). *J*: Representative immunoblot. The number of individual mice per group was 7–30. Normality tests were performed using the D'Agostino and Pearson test. Statistical analyses were performed using Kruskal-Wallis test and Dunn multiple comparisons test in *B–D*, *F*, and *G*, one-way ANOVA followed by Tukey multiple comparisons test in *E*, and Mann-Whitney *U* test in *H* and *I*. Outliers were removed based on Grubbs test with $\alpha = 0.01$: (1,0,0) data points were removed in *F*, (0,1) data points were removed in *H*, (0,1) data points were removed in *I*, and no data points were removed in *B–E* and *G*. AU, arbitrary unit.

with hematopoietic GSDMD deficiency (Fig. 2*I*). It is possible that other cell death pathways are activated in GSDMD-deficient cells (36) or that GSDMD deficiency results in increased inflammasome activation through a feedback loop mediated by the N-terminal GSDMD fragment (37). Such effects might be masked by the increased necrosis in diabetes.

To verify that whole-body deletion of GSDMD results in protection from atherosclerosis development, as has been reported by others (27), a control cohort of whole-body GSDMD-deficient mice and wild-type littermate controls were injected with LDLR ASO and fed an HFHS diet to initiate and promote atherosclerosis (Supplementary Fig. 1A). Whole-body GSDMD deficiency resulted in reduced lesion area, consistent with a previous study (27), and reduced relative necrotic core area (Supplementary Fig. 1*B–D*).

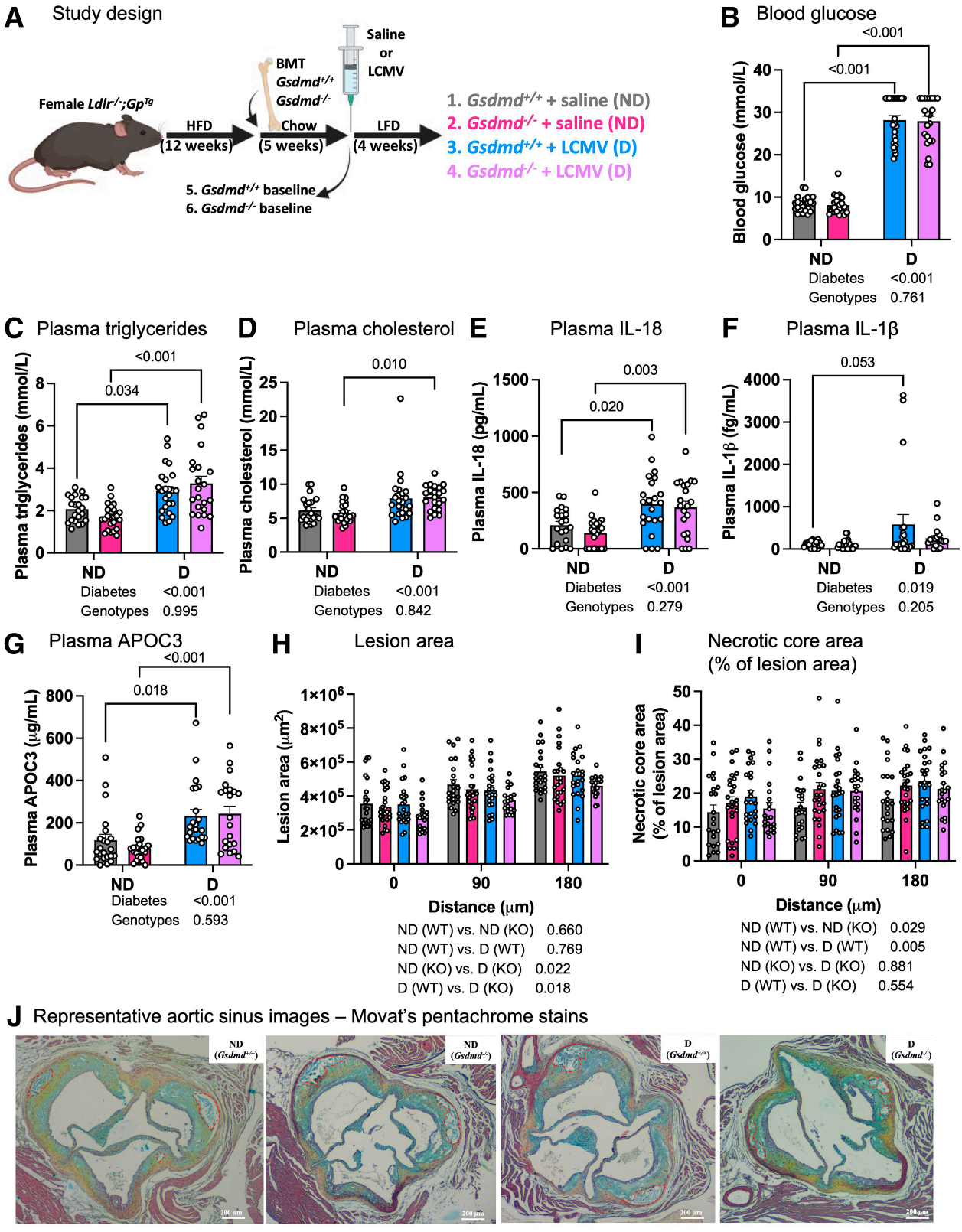

Figure 2—Hematopoietic GSDMD deficiency does not prevent the effect of diabetes on lesion necrotic core expansion. Female $Ldlr^{-/-}$;Gp^{Tg} mice were maintained on an HFD for 12 weeks to allow the formation of preexisting lesions. The mice were then lethally irradiated and received bone marrow cells from animals with and without GSDMD deficiency. The animals were maintained on a chow diet and recovered for 5 weeks. Mice were rendered diabetic (D) with LCMV. Saline was used as a control (nondiabetic [ND]). At the onset of diabetes, the animals were switched to a semipurified LFD with no added cholesterol and maintained for 4 weeks. A subset of animals was euthanized after 5 weeks of recovery to evaluate lesion morphology before diabetes (baseline). *A*: Schematic of the study design. *B*: Blood glucose levels. Glucose values >33.3 mmol/L are

Nonhematopoietic GSDMD Contributes to the Release of Circulating IL-18 and IL-1β

To investigate whether hematopoietic GSDMD is responsible for the release of IL-1β and IL-18 to plasma in vivo, animals with and without whole-body or hematopoietic GSDMD deficiency were treated with ultrapure LPS and ATP for acute inflammasome activation in the peritoneal cavity (Fig. 3*A* and *D*). Animals with whole-body GSDMD deficiency exhibited markedly suppressed plasma IL-1β and IL-18 levels upon inflammasome activation (Fig. 3*B* and *C* and Supplementary Fig. 8). There were no marked differences in plasma IL-18 responses between male and female mice or between C57BL/6 mice and $Ldlr^{-/-}$;Gp^{Tg} mice to LPS and ATP stimulation (Supplementary Fig. 8). These findings concur with previous studies demonstrating that GSDMD contributes to the release of IL-1β and IL-18 (26). However, hematopoietic GSDMD deficiency failed to suppress plasma IL-1β and IL-18 levels upon inflammasome activation (Fig. 3*E* and *F*), consistent with the lack of plasma IL-1β and IL-18 reduction in diabetic mice with hematopoietic GSDMD deficiency (Fig. 2*E* and *F*). Our findings suggest that the release of IL-18 and IL-1β to the plasma compartment might be mediated via nonhematopoietic cells in this model of acute inflammasome activation.

To further investigate whether diabetes induces inflammasome activation in macrophages through a GSDMD-dependent pathway, we analyzed inflammasome activation in $F4/80^+$ peritoneal macrophages. These studies confirmed the successful deletion of GSDMD in $F4/80^+$ peritoneal cavity macrophages. We were unable to detect increased levels of cleaved (active) forms of GSDMD and caspase-1 in macrophage lysates from diabetic mice. However, diabetes increased levels of cleaved GSDMD and caspase-1 in the peritoneal cavity fluid through a mechanism that was independent of hematopoietic GSDMD deficiency (Supplementary Fig. 9). These findings suggest that while inflammasome activation may occur in macrophages (or possibly in other cell types) in diabetic mice, the release of cleaved caspase-1 is independent of GSDMD.

Hematopoietic AIM2 and NLRP3 Deficiencies Do Not Alter Blood Glucose, Serum Lipids, IL-1β, or IL-18 in Diabetic Mice, but Hematopoietic NLRP3 Deficiency Results in Reduced Serum APOC3 Levels

Previous studies demonstrated that hematopoietic inflammasome activation can promote lesion progression in other models (22–25), which prompted the investigation of whether hematopoietic AIM2, NLRP3, and DKOs, upstream of GSDMD, can prevent early atherosclerosis initiation and progression under diabetic conditions. Female $Ldlr^{-/-}$ mice received bone marrow transplants from donors with AIM2 deficiency, NLRP3 deficiency, or DKOs before induction of diabetes and Western diet feeding for 8 weeks (Fig. 4*A*). Hematopoietic inflammasome deficiencies did not significantly affect blood glucose, serum triglycerides, serum cholesterol levels, serum IL-1β or IL-18 levels (Fig. 4*B–F*), consistent with the lack of effect from hematopoietic GSDMD deficiency (Fig. 2*B–F*). However, hematopoietic NLRP3 deficiency resulted in lower serum levels of APOC3, an effect observed both in diabetic mice with NLRP3 deficiency and in DKO (Fig. 4*G*).

Hematopoietic AIM2 and NLRP3 Deficiencies Suppress the Aortic Sinus Lesion Area but Not the Relative Necrotic Core Area in Diabetic Mice

Diabetic mice with hematopoietic deletions of NLRP3 and/or AIM2 had reduced sinus lesion size (Fig. 4*H*), which is consistent with previous studies (22–25). However, the hematopoietic deletions of NLRP3 and AIM2 failed to reduce the relative necrotic core area (Fig. 4*I*). Neither NLRP3 nor AIM2 deficiency resulted in changes in lesion $Mac2^+$ area or α-SMA^+ area (Supplementary Fig. 10). Thus, hematopoietic NLRP3 and AIM2 inflammasome activation contributes to lesion development (lesion area) but not to a relative expansion of the necrotic core area or marked changes in cell type composition in diabetic mice at an 8-week time point of atherosclerosis. Importantly, although the STZ diabetic mice in this experiment were less severely diabetic than the LCMV diabetic mice (as shown by their lower blood glucose levels) and had higher serum cholesterol than the LCMV model because of the Western diet, there were no significant differences between the STZ model and the LCMV model of type 1 diabetes in triglycerides, IL-18, IL-1β, sinus lesion area, relative necrotic core area, or overall lesion severity (Supplementary Table 8).

Diabetes Increases APOC3 and APOE Accumulation in the Aortic Sinus Through a GSDMD-Independent Mechanism

To further investigate the potential culprit responsible for necrotic core expansion in diabetes-accelerated advanced atherosclerosis, aortic sinuses harvested from animals with and without diabetes and/or hematopoietic GSDMD deficiency were immunostained for APOC3, APOB, and APOE, apolipoproteins present on TRLs. Our data show that

expressed as 33.3 mmol/L. *C*: Plasma triglyceride levels. *D*: Plasma cholesterol levels. *E*: Plasma IL-18 levels. *F*: Plasma IL-1β levels. *G*: Plasma APOC3 levels. *H*: Aortic sinus lesion area; 0 μm represents the first appearance of the three aortic valve leaflets. *I*: Aortic sinus percent necrotic core area calculated as necrotic core area / lesion area. *J*: Representative aortic sinus lesions stained with Movat pentachrome stain. Representative necrotic core areas are circled in red. Data are mean ± SEM (n = 19–25 mice/group). Statistical analyses were performed by two-way ANOVA followed by Tukey multiple comparisons test. In *B–G*, lines between two groups indicate P values calculated by multiple comparisons test, and the text underneath the graphs indicates overall group effects (P values) as calculated by two-way ANOVA. In *H* and *I*, the text underneath the graphs indicates group effects (P values) as calculated by the multiple comparisons test. Outliers were removed based on Grubbs test with α = 0.01: (0,0,1,0) data points were removed in *D*, (0,0,1,1) data points were removed in *F*, (0,0,1,0) data points were removed in *G*, (0,0,0,0,0,0,0,1,1,1,0,1) data points were removed in *H*, and no data points were removed in *B*, *C*, *E*, and *I*. BMT, bone marrow transplant; KO, knockout; WT, wild type.

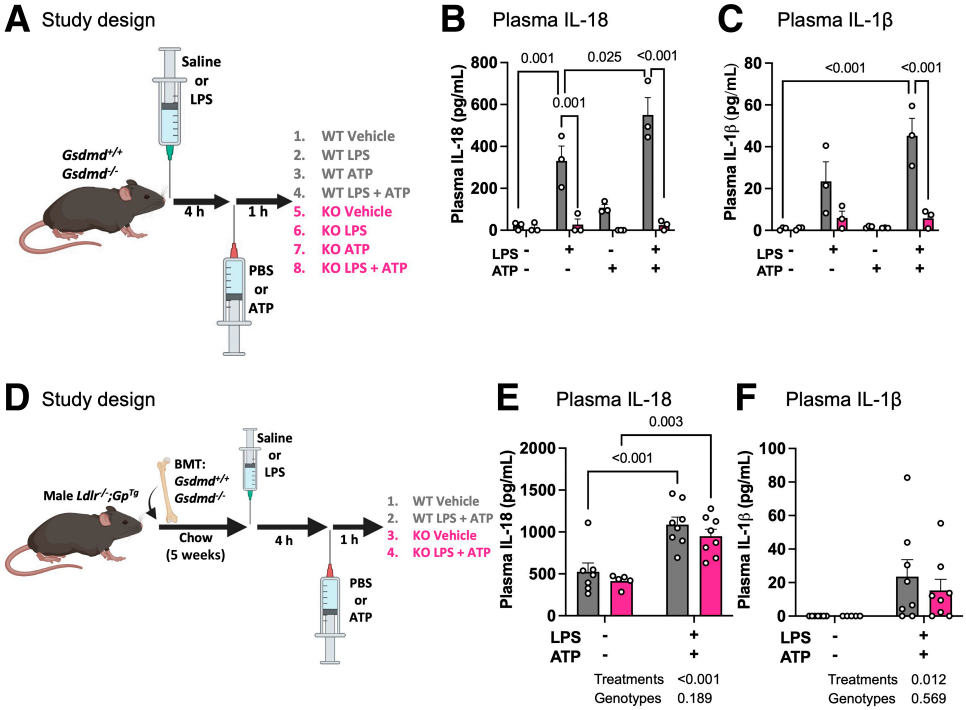

Figure 3— Full-body but not hematopoietic GSDMD deficiency contributes to the release of circulating IL-18 and IL-1β. *A–C*: Male and female mice with and without whole-body GSDMD deficiency received i.p. injections of ultrapure LPS, ATP, or saline controls to induce inflammasome activation. *A*: Schematic of the study design. *B*: Plasma IL-18. *C*: Plasma IL-1β. Data are mean ± SEM (n = 3 mice/group in *B* and *C*). Statistical analyses were performed using two-way ANOVA followed by Tukey multiple comparisons test. *D–F*: Male $Ldlr^{-/-}$;Gp^{Tg} mice were lethally irradiated and received bone marrow cells from animals with and without GSDMD deficiency. The animals were maintained on a chow diet and recovered for 5 weeks. The mice were then injected with and without ultrapure LPS and ATP after 5 weeks of recovery. *D*: Schematic of the study design. *E*: Plasma IL-18. *F*: Plasma IL-1β. Data are mean ± SEM (n = 7, 5, 8, and 8 mice/group in *E* and *F*). Statistical analyses were performed using two-way ANOVA followed by Tukey multiple comparisons test. In *B* and *C* and *E* and *F*, the lines between two groups indicate P values between the groups as calculated by multiple comparisons test. In *E* and *F*, the text underneath the graphs indicates overall group effects (P values) as calculated by two-way ANOVA. Outliers were removed based on Grubbs test with $\alpha = 0.01$: no data points were removed in *B* and *C* and *E* and *F*. BMT, bone marrow transplant; KO, knockout; WT, wild type.

diabetes not only elevates plasma APOC3 levels (Figs. 1*F* and 2*G*) but also increases lesional APOC3 accumulation, as measured by $APOC3^{+}$ immunoreactivity (Fig. 5*A* and *F*). Lesional $APOE^{+}$ immunoreactivity and lesion area positive for both APOB and APOE were also increased under diabetic conditions (Fig. 5*B–E*), consistent with the known APOC3 effect in inhibiting the clearance of TRLs and their remnants (6–8). There was no effect of hematopoietic GSDMD deficiency. Likewise, diabetic mice with hematopoietic DKO showed no significant differences in either lesional $APOC3^{+}$ or $APOB^{+}APOE^{+}$ immunoreactivities (Supplementary Fig. 10). Together, these findings suggest that APOC3, through abnormal metabolism of TRLs and their remnants, might be indirectly responsible for accelerating necrotic core progression under diabetic conditions, consistent with our previous studies (14,31).

DISCUSSION

Atherosclerosis is a chronic inflammatory disease that can involve hematopoietic inflammasome activation. Previous studies have demonstrated that hematopoietic deletion of essential inflammasome components confers atheroprotection under conditions associated with increased inflammasome activation (22–25). With the clinical effectiveness of IL-1β inhibition in preventing CVD events in individuals with and without diabetes (13), the presence of a similar pathological mechanism in diabetes-associated atherosclerosis becomes a plausible hypothesis. The involvement of inflammasome pathways in diabetes-associated atherosclerosis is further supported by studies demonstrating that APOC3 predicts future CVD events in individuals with type 1 diabetes (14–16) and that delipidated APOC3 can induce alternative NLRP3 inflammasome activation in human monocytes (17,18). Moreover, systemic inhibition of the NLRP3 inflammasome pathway using a small-molecule inhibitor prevented atherosclerosis in diabetic mice (4). We can now show that mice with type 1 diabetes do exhibit increased inflammasome activation, measured as elevated plasma IL-18 and IL-1β, and increased levels of cleaved caspase-1 in the peritoneal cavity interstitial fluid. Furthermore, our study provides strong evidence that in diabetic mice hematopoietic NLRP3 and AIM2, as well as GSDMD, contribute to lesion size but not to a relative increase in necrotic core expansion a feature associated with clinical events in humans (12). Deletion of the cholesterol exporters ABCA1 and ABCG1 in myeloid cells is known to activate the NLRP3 inflammasome (22). Reduced expression of

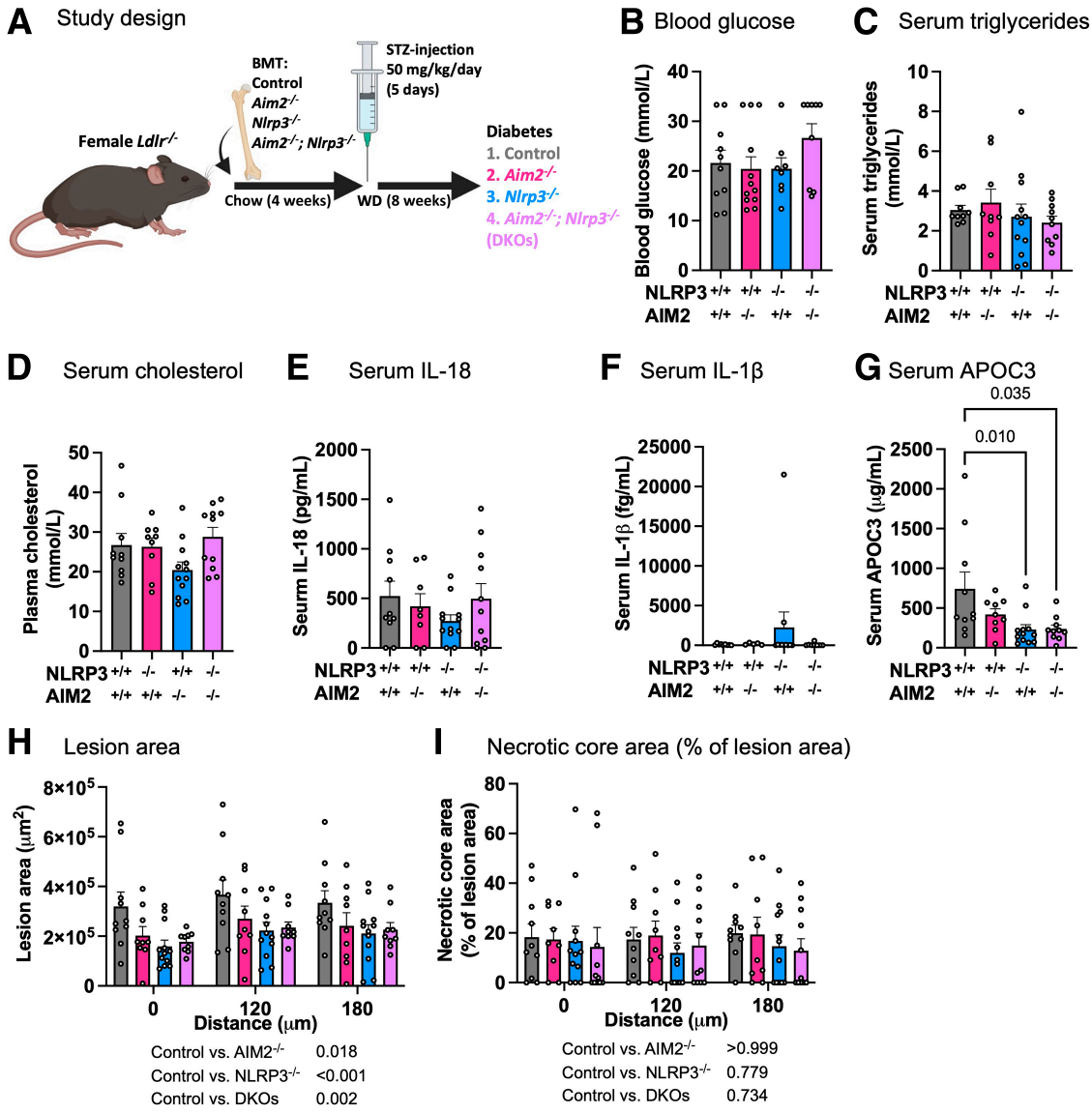

Figure 4—Hematopoietic AIM2, NLRP3, and DKO contribute to lesion area but not necrotic core area in the setting of diabetes. Female *Ldlr*$^{-/-}$ mice were lethally irradiated and received bone marrow from mice with and without Nlrp3 deficiency (*Nlrp3*$^{-/-}$), Aim2 deficiency (*Aim2*$^{-/-}$), or DKO. The animals were recovered on chow for 4 weeks before diabetes was induced with 5 days of STZ injections (50 mg/kg/day). Animals were maintained on a Western diet (WD) for 8 weeks. *A*: Schematic of the study design. *B*: Blood glucose levels. Glucose values >33.3 mmol/L are expressed as 33.3 mmol/L. Animals with average blood glucose <13.9 mmol/L were removed from the study. *C*: Serum triglyceride levels. *D*: Serum cholesterol levels. *E*: Serum IL-18 levels. *F*: Serum IL-1β levels. *G*: Serum APOC3 levels. *H*: Aortic sinus lesion area where 0 μm represents the first appearance of the three aortic valve leaflets. *I*: Aortic sinus necrotic core area calculated as percent of lesion area. Data are mean ± SEM (*n* = 9–12 mice/group). Statistical analyses were performed using Kruskal-Wallis test and Dunn multiple comparisons test in *B*–*G* and using two-way ANOVA followed by Tukey multiple comparisons test in *H* and *I*. Normality test was performed using D'Agostino and Pearson test. In *H* and *I*, the text underneath the graphs indicates *P* values between the groups as calculated by the multiple comparisons test. Outliers were removed based on Grubbs test with $\alpha = 0.01$: (1,1,1,1) data points were removed in *F*, and no data points were removed in *B*–*E* and *G* and *H*. BMT, bone marrow transplant.

these transporters in macrophages in the setting of diabetes (38,39) might therefore contribute to NLRP3 activation. The AIM2 inflammasome, which is potentially activated by cytosolic double-stranded DNA from phagocytosed dead cells or damaged nuclei or mitochondria (40), has not previously been shown to contribute to atherosclerosis in diabetes. Although the mechanism whereby diabetes activates the AIM2 inflammasome needs further investigation, an interesting possibility is that mitochondrial dysfunction in macrophages from diabetic mice (41) could contribute to the activation of the AIM2 inflammasome. Oxidative DNA damage has been implicated in AIM2 activation and accelerated atherosclerosis associated with clonal hematopoiesis (25).

Despite the increased inflammasome activation in diabetic mice, our results indicate that hematopoietic GSDMD deletion does not reduce the release of IL-1β and IL-18 to plasma. The lack of reduction in plasma IL-1β and IL-18 levels in animals with hematopoietic GSDMD deficiency

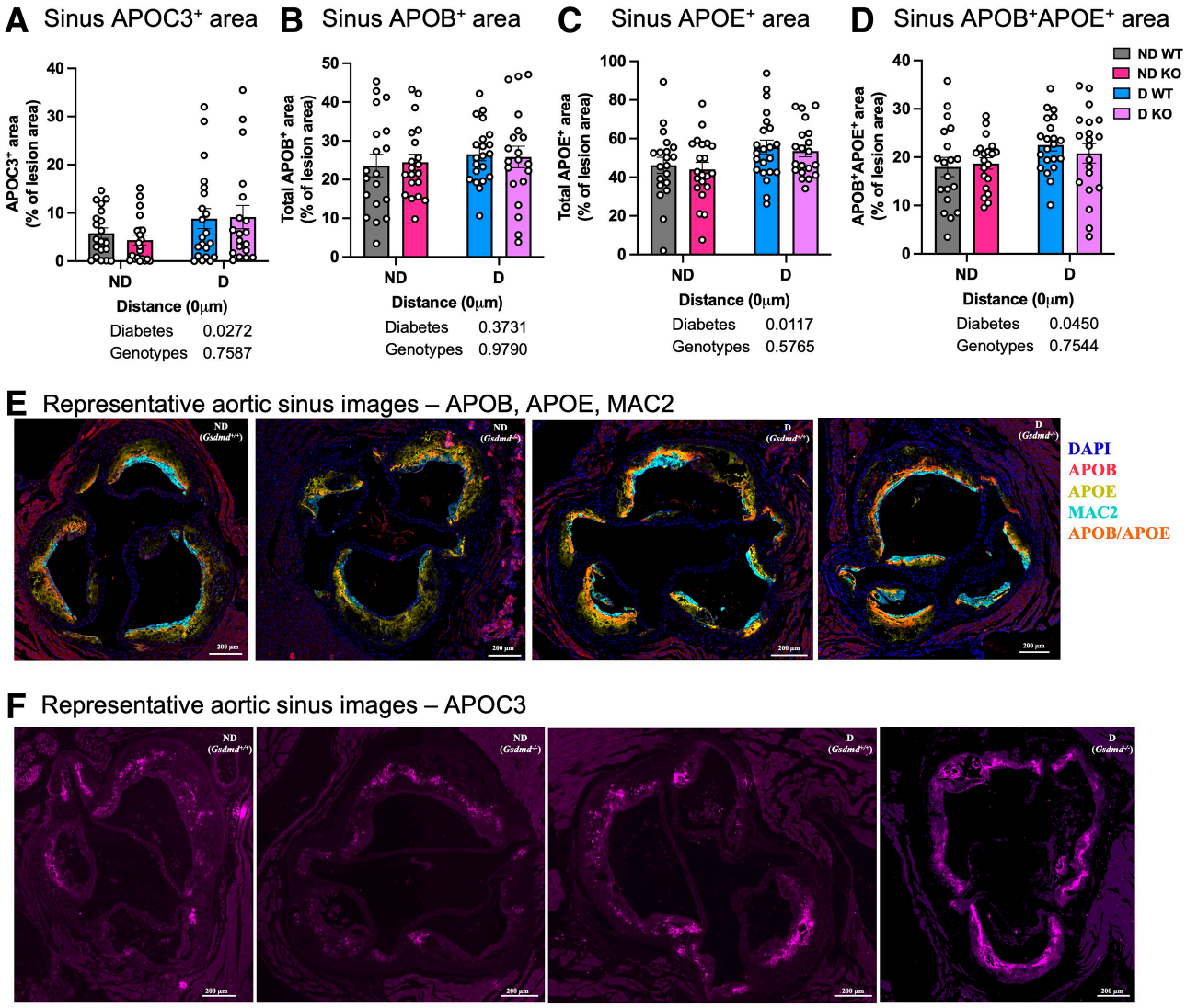

Figure 5—Diabetes increases APOC3 and APOE accumulation in aortic sinus lesions, but hematopoietic GSDMD deficiency has no effect. Female *Ldlr*$^{-/-}$;*Gp*^{Tg} mice were maintained on an HFD for 12 weeks to allow the formation of preexisting lesions. Mice were lethally irradiated and received bone marrow cells from animals with and without GSDMD deficiency. The animals were maintained on a chow diet and recovered for 5 weeks. Mice were rendered diabetic (D) with LCMV. Saline was used as a control (nondiabetic [ND]). At the onset of diabetes, the animals were switched to a semipurified LFD with no added cholesterol and were maintained for 4 weeks. *A*: Aortic sinus APOC3^{+} area. *B*: Aortic sinus total APOB^{+} area. *C*: Aortic sinus total APOE^{+} area. *D*: Aortic sinus APOB^{+}APOE^{+} area. *E*: Representative aortic sinuses with Mac2, APOB, and APOE staining. *F*: Representative aortic sinuses with APOC3 staining. Immunofluorescence staining of Mac2, APOC3, APOB, and APOE were conducted at 0 μm. Data are mean ± SEM (n = 20, 21, 21, and 20 mice/group in *A*; 19, 20, 21, 20 mice/group in *B* and *D*; and 20, 21, 22, and 20 mice/group in *C*). Statistical analyses were performed by two-way ANOVA followed by Tukey multiple comparisons test in *A*–*D*. The text underneath the graphs indicates overall group effects (P values) as calculated by two-way ANOVA. Outliers were removed based on Grubbs test with α = 0.01: (0,0,0,1) data points were removed in *A*, and no data points were removed in *B*–*D*. KO, hematopoietic GSDMD knockout; WT, wild type.

suggests that IL-1β and IL-18 that reach the plasma pool are secreted from hematopoietic cells via pathways independent of GSDMD, such as through gasdermin E (26), or potentially from nonhematopoietic cells. However, measurements of plasma levels of IL-1β and IL-18 might not capture local effects in tissues or on lesion development, especially since IL-18 is expressed by nearly all epithelial cells and keratinocytes, in addition to myeloid cells (42).

The inability of hematopoietic GSDMD deficiency to suppress plasma IL-1β and IL-18 levels provided an opportunity to study the effects of the GSDMD pyroptotic pathway on diabetes-associated atherosclerosis independent of systemic proinflammatory cytokine suppression. Macrophage cell death is considered a major contributor to lesional necrotic core formation (26); however, whether pyroptosis contributes to necrotic core formation under diabetic conditions has remained unexplored. Pyroptosis is defined as cell death mediated by GSDMD (43). Because there are many other types of cell death, pyroptosis can currently only be selectively measured in vivo as cell death prevented by GSDMD deficiency (26). Consistent with previous studies (14,31), diabetes accelerated aortic sinus

necrotic core expansion without increasing the lesion area of preexisting lesions in our study. However, targeting hematopoietic GSDMD did not affect the relative necrotic core area, suggesting that this aspect of diabetes-accelerated atherosclerosis is governed by mechanisms independent of hematopoietic GSDMD-mediated pyroptosis.

Altogether, our study provides evidence demonstrating that while hematopoietic NLRP3, AIM2, and GSDMD do not play critical roles in necrotic core expansion, they do contribute to overall lesion size in diabetic mice. The reasons for the different results on the role of hematopoietic NLRP3, AIM2, and GSDMD on atherosclerosis in different mouse models (22–25,44,45) are uncertain but could be related to female-specific effects (29) or the presence of different factors that lead to increased inflammasome activation. Together, these studies suggest a greater effect of hematopoietic inflammasome activation in mice or humans with additional conditions or mutations that promote inflammasome activation, such as diabetes or clonal hematopoiesis associated with the *JAK2* ^{V617F} variant (25).

Our results suggest that the relative necrotic core expansion in lesions of diabetic mice involves a mechanism independent of inflammasome activation and pyroptosis. There are multiple risk factors associated with increased CVD risk in individuals with diabetes (46), one of which could be abnormal metabolism of TRLs (6–8). We have previously shown that silencing of APOC3 prevents lesion initiation, necrotic core expansion, and accumulation of lesion APOC3 immunoreactivity in diabetic mice (14). Consistently, studies in people have shown a correlation between plasma APOC3 and necrotic core volume (47). The current study demonstrates that diabetes increases the accumulation of immunoreactive APOC3 and APOE, as well as colocalization of APOE and APOB in the aortic sinus. TRLs and their remnants are APOB lipoproteins that carry APOC3 and APOE (8). It is therefore tempting to speculate that the increased necrotic core size in diabetic mice could be due to accumulation of TRLs or TRL remnants, which are readily taken up by macrophages (48) and endothelial cells (49). However, some of the APOE is derived from cells in the lesion rather than from the circulation. The exact mechanism whereby increased APOC3 in diabetes promotes lesion necrotic core expansion needs further investigation but could involve indirect effects mediated by TRL remnants in endothelial cells, smooth muscle cells, or lesion immune cell populations. It is possible that other forms of cell death, such as ferroptosis or necroptosis (26), could contribute to APOC3-mediated necrotic core expansion in the setting of diabetes.

Our study sheds further light on the links between NLRP3 and APOC3. APOC3 can activate an alternative NLRP3 inflammasome pathway in both human and mouse monocytes but only in its delipidated form (17,18). When APOC3 is bound to lipid particles, which it is in the circulation, this effect is lost (18). Moreover, silencing of APOC3 did not lower plasma IL-18 levels in our mouse model of type 1 diabetes (18). It is therefore unlikely that APOC3 acts upstream of NLRP3 inflammasome activation. However, there is an association between an *NLRP3* variant that results in increased NLRP3 activation and plasma APOC3 levels (50). Our finding that serum APOC3 levels are lower in diabetic mice with hematopoietic NLRP3 deficiency raises the possibility that NLRP3 might act upstream of APOC3 rather than downstream of APOC3 in vivo. It is, for example, possible that NLRP3 activation in hepatic leukocytes results in increased APOC3 production or reduced APOC3 clearance. Furthermore, since the decrease in APOC3 levels (from 740 to 420 μg/mL) that resulted from NLRP3 deficiency did not lead to a decrease in necrotic core area, this suggests that a more extensive reduction in APOC3 is required to prevent necrotic core expansion or that the association between plasma APOC3 and necrotic core area does not indicate direct causation.

Our study has several limitations. Although the two different type 1 diabetes models exhibited similar levels of plasma IL-1β and IL-18 and similar lesion sizes and severity, direct quantitative comparisons are not possible. For example, in the STZ diabetes experiment, hematopoietic NLRP3 and AIM2 deficiencies were present during both lesion initiation and progression, whereas the GSDMD experiment was designed to investigate effects on preexisting lesions. Moreover, nondiabetic controls might have been informative in the STZ experiment, as would inclusions of male mice in all experiments. Also, it is likely that IL-1β and IL-18 act locally within the lesion. Direct measurements of inflammasome activation and release of mature IL-1β and IL-18 in lesions of atherosclerosis are hampered by the lack of antibodies able to distinguish mature and proforms of these cytokines.

Despite these limitations, our findings demonstrate that hematopoietic NLRP3, AIM2, and GSDMD promote lesion development in the setting of diabetes but increased necrotic core expansion is independent of hematopoietic GSDMD or pyroptosis. Further studies are needed to clarify the relative importance of inflammasome activation and APOC3-containing TRL remnants in cardiovascular complications of diabetes.

Acknowledgments. The authors thank Dr. Adam Mullick (Ionis Pharmaceuticals) for the LDLR ASO used in this study. Schematics were created using BioRender (https://www.biorender.com).

Funding. This study was supported by National Heart, Lung, and Blood Institute grants R35HL150754, P01HL151328, and R01HL161829 (to K.E.B.) and a predoctoral fellowship award from the American Heart Association (828090 to C.-C.H.).

Duality of Interest. K.E.B. serves on a scientific advisory board of Esperion Therapeutics. A.R.T. is a consultant or scientific advisory board member of Staten Biotechnology, 1016 Bio, Commonwealth Serum Laboratories, and Beren Pharmaceuticals. No other potential conflicts of interest relevant to this article were reported.

Author Contributions. C.-C.H. performed the experiments, analyzed data, and wrote the manuscript. T.P.F., J.E.K., V.K., F.K., and J.T. performed a subset of experiments and analyzed corresponding data. A.R.T. provided advice and samples and edited the manuscript. K.E.B. designed and directed the study.

All authors reviewed the manuscript and provided final approval for submission. K.E.B. is the guarantor of this work and, as such, had full access to all the data in the study and takes responsibility for the integrity of the data and the accuracy of the data analysis.

Prior Presentation. Parts of this study were presented in an abstract form at the Vascular Discovery 2022 Scientific Sessions of the American Heart Association, Seattle, WA, 11–14 May 2022.

References

1. Tsao CW, Aday AW, Almarzooq ZI, et al. Heart disease and stroke statistics-2022 update: a report from the American Heart Association. Circulation 2022; 145:e153–e639
2. Nishikawa T, Edelstein D, Du XL, et al. Normalizing mitochondrial superoxide production blocks three pathways of hyperglycaemic damage. Nature 2000;404:787–790
3. Senatus L, MacLean M, Arivazhagan L, et al. Inflammation meets metabolism: roles for the receptor for advanced glycation end products axis in cardiovascular disease. Immunometabolism 2021;3:e210024
4. Sharma A, Choi JSY, Stefanovic N, et al. Specific NLRP3 inhibition protects against diabetes-associated atherosclerosis. Diabetes 2021;70:772–787
5. Kanter JE, Hsu CC, Bornfeldt KE. Monocytes and macrophages as protagonists in vascular complications of diabetes. Front Cardiovasc Med 2020;7:10
6. Bornfeldt KE. The remnant lipoprotein hypothesis of diabetes-associated cardiovascular disease. Arterioscler Thromb Vasc Biol 2022;42:819–830
7. Tall AR, Thomas DG, Gonzalez-Cabodevilla AG, Goldberg IJ. Addressing dyslipidemic risk beyond LDL-cholesterol. J Clin Invest 2022;132:e148559
8. Chait A, Ginsberg HN, Vaisar T, Heinecke JW, Goldberg IJ, Bornfeldt KE. Remnants of the triglyceride-rich lipoproteins, diabetes, and cardiovascular disease. Diabetes 2020;69:508–516
9. Moore KJ, Tabas I. Macrophages in the pathogenesis of atherosclerosis. Cell 2011;145:341–355
10. Libby P, Buring JE, Badimon L, et al. Atherosclerosis. Nat Rev Dis Primers 2019;5:56
11. Burke AP, Kolodgie FD, Zieske A, et al. Morphologic findings of coronary atherosclerotic plaques in diabetics: a postmortem study. Arterioscler Thromb Vasc Biol 2004;24:1266–1271
12. Bentzon JF, Otsuka F, Virmani R, Falk E. Mechanisms of plaque formation and rupture. Circ Res 2014;114:1852–1866
13. Ridker PM, Everett BM, Thuren T, et al.; CANTOS Trial Group. Antiinflammatory therapy with canakinumab for atherosclerotic disease. N Engl J Med 2017;377: 1119–1131
14. Kanter JE, Shao B, Kramer F, et al. Increased apolipoprotein C3 drives cardiovascular risk in type 1 diabetes. J Clin Invest 2019;129:4165–4179
15. Basu A, Bebu I, Jenkins AJ, et al.; Diabetes Control Complications Trial/ Epidemiology of Diabetes Interventions Complications Research Group. Serum apolipoproteins and apolipoprotein-defined lipoprotein subclasses: a hypothesis-generating prospective study of cardiovascular events in T1D. J Lipid Res 2019; 60:1432–1439
16. Jansson Sigfrids F, Stechemesser L, Dahlström EH, et al.; FinnDiane Study Group. Apolipoprotein C-III predicts cardiovascular events and mortality in individuals with type 1 diabetes and albuminuria. J Intern Med 2022;291:338–349
17. Zewinger S, Reiser J, Jankowski V, et al. Apolipoprotein C3 induces inflammation and organ damage by alternative inflammasome activation. Nat Immunol 2020;21:30–41
18. Hsu CC, Shao B, Kanter JE, et al. Apolipoprotein C3 induces inflammasome activation only in its delipidated form. Nat Immunol 2023;24:408–411
19. Lee HM, Kim JJ, Kim HJ, Shong M, Ku BJ, Jo EK. Upregulated NLRP3 inflammasome activation in patients with type 2 diabetes. Diabetes 2013;62: 194–204
20. Henriksbo BD, Lau TC, Cavallari JF, et al. Fluvastatin causes NLRP3 inflammasome-mediated adipose insulin resistance. Diabetes 2014;63:3742–3747
21. Henriksbo BD, Tamrakar AK, Xu J, et al. Statins promote interleukin-1β-dependent adipocyte insulin resistance through lower prenylation, not cholesterol. Diabetes 2019;68:1441–1448
22. Westerterp M, Fotakis P, Ouimet M, et al. Cholesterol efflux pathways suppress inflammasome activation, NETosis, and atherogenesis. Circulation 2018;138:898–912
23. Tumurkhuu G, Shimada K, Dagvadorj J, et al. Ogg1-dependent DNA repair regulates NLRP3 inflammasome and prevents atherosclerosis. Circ Res 2016;119:e76–e90
24. Zhang X, McDonald JG, Aryal B, et al. Desmosterol suppresses macrophage inflammasome activation and protects against vascular inflammation and atherosclerosis. Proc Natl Acad Sci U S A 2021;118:e2107682118
25. Fidler TP, Xue C, Yalcinkaya M, et al. The AIM2 inflammasome exacerbates atherosclerosis in clonal haematopoiesis. Nature 2021;592:296–301
26. Puylaert P, Zurek M, Rayner KJ, De Meyer GRY, Martinet W. Regulated necrosis in atherosclerosis. Arterioscler Thromb Vasc Biol 2022;42:1283–1306
27. Opoku E, Traughber CA, Zhang D, et al. Gasdermin D mediates inflammation-induced defects in reverse cholesterol transport and promotes atherosclerosis. Front Cell Dev Biol 2021;9:715211
28. Renard CB, Kramer F, Johansson F, et al. Diabetes and diabetes-associated lipid abnormalities have distinct effects on initiation and progression of atherosclerotic lesions. J Clin Invest 2004;114:659–668
29. Chen S, Markman JL, Shimada K, et al. Sex-specific effects of the Nlrp3 inflammasome on atherogenesis in LDL receptor-deficient mice. JACC Basic Transl Sci 2020;5:582–598
30. Kayagaki N, Stowe IB, Lee BL, et al. Caspase-11 cleaves gasdermin D for non-canonical inflammasome signalling. Nature 2015;526:666–671
31. Shimizu-Albergine M, Basu D, Kanter JE, et al. CREBH normalizes dyslipidemia and halts atherosclerosis in diabetes by decreasing circulating remnant lipoproteins. J Clin Invest 2021;131:e153285
32. Subramanian S, Han CY, Chiba T, et al. Dietary cholesterol worsens adipose tissue macrophage accumulation and atherosclerosis in obese LDL receptor-deficient mice. Arterioscler Thromb Vasc Biol 2008;28:685–691
33. Stary HC, Chandler AB, Dinsmore RE, et al. A definition of advanced types of atherosclerotic lesions and a histological classification of atherosclerosis. A report from the Committee on Vascular Lesions of the Council on Arteriosclerosis, American Heart Association. Circulation 1995;92:1355–1374
34. Nagareddy PR, Murphy AJ, Stirzaker RA, et al. Hyperglycemia promotes myelopoiesis and impairs the resolution of atherosclerosis. Cell Metab 2013; 17:695–708
35. Swirski FK, Libby P, Aikawa E, et al. Ly-6Chi monocytes dominate hypercholesterolemia-associated monocytosis and give rise to macrophages in atheromata. J Clin Invest 2007;117:195–205
36. Tonnus W, Maremonti F, Belavgeni A, et al. Gasdermin D-deficient mice are hypersensitive to acute kidney injury. Cell Death Dis 2022;13:792
37. Hu Y, Jiang Y, Li S, et al. The gasdermin D N-terminal fragment acts as a negative feedback system to inhibit inflammasome-mediated activation of caspase-1/11. Proc Natl Acad Sci U S A 2022;119:e2210809119
38. Tang C, Kanter JE, Bornfeldt KE, Leboeuf RC, Oram JF. Diabetes reduces the cholesterol exporter ABCA1 in mouse macrophages and kidneys. J Lipid Res 2010;51:1719–1728
39. Mauldin JP, Nagelin MH, Wojcik AJ, et al. Reduced expression of ATP-binding cassette transporter G1 increases cholesterol accumulation in macrophages of patients with type 2 diabetes mellitus. Circulation 2008;117:2785–2792
40. Soehnlein O, Tall AR. AIMing 2 treat atherosclerosis. Nat Rev Cardiol 2022;19:567–568
41. Matsuura Y, Shimizu-Albergine M, Barnhart S, et al. Diabetes suppresses glucose uptake and glycolysis in macrophages. Circ Res 2022;130:779–781
42. Dinarello CA, Novick D, Kim S, Kaplanski G. Interleukin-18 and IL-18 binding protein. Front Immunol 2013;4:289
43. Shi J, Zhao Y, Wang K, et al. Cleavage of GSDMD by inflammatory caspases determines pyroptotic cell death. Nature 2015;526:660–665

44. Duewell P, Kono H, Rayner KJ, et al. NLRP3 inflammasomes are required for atherogenesis and activated by cholesterol crystals. Nature 2010;464:1357–1361
45. Hendrikx T, Jeurissen ML, van Gorp PJ, et al. Bone marrow-specific caspase-1/11 deficiency inhibits atherosclerosis development in Ldlr(-/-) mice. FEBS J 2015;282:2327–2338
46. Eckel RH, Bornfeldt KE, Goldberg IJ. Cardiovascular disease in diabetes, beyond glucose. Cell Metab 2021;33:1519–1545
47. Ohwada T, Sakamoto T, Suzuki S, et al. Apolipoprotein C3 and necrotic core volume are correlated but also associated with future cardiovascular events. Sci Rep 2022;12:14554
48. Van Lenten BJ, Fogelman AM, Jackson RL, Shapiro S, Haberland ME, Edwards PA. Receptor-mediated uptake of remnant lipoproteins by cholesterol-loaded human monocyte-macrophages. J Biol Chem 1985;260: 8783–8788
49. Cabodevilla AG, Tang S, Lee S, et al. Eruptive xanthoma model reveals endothelial cells internalize and metabolize chylomicrons, leading to extravascular triglyceride accumulation. J Clin Invest 2021;131:e145800
50. Zewinger S, Reiser J, Jankowski V, et al. Reply to: apolipoprotein C3 induces inflammasome activation only in its delipidated form. Nat Immunol 2023;24:412–413